Selective Depolymerization for Sculpting Polymethacrylate Molecular Weight Distributions

Ariana M. Tamura‡, Kevin A. Stewart‡, James B. Young‡, Nathan B. Wei, Alexander J. Cantor, Brent S. Sumerlin*

*Correspondence: sumerlin@chem.ufl.edu

George & Josephine Butler Polymer Research Laboratory, Center for Macromolecular Science & Engineering, Department of Chemistry, University of Florida, Gainesville, FL 32611, USA

‡These authors contributed equally.

KEYWORDS: Depolymerization, reversible-deactivation radical polymerization, polymer blends, shear rheology, data encryption

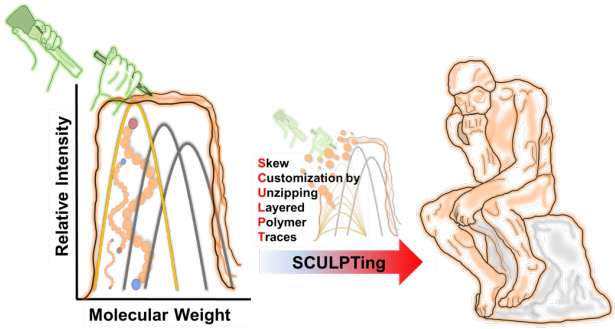

ABSTRACT: Chain-end reactivation of polymethacrylates generated by reversible-deactivation radical polymerization (RDRP) has emerged as a powerful tool for triggering depolymerization at significantly milder temperatures than traditionally employed. In this study, we demonstrate how the facile depolymerization of poly(butyl methacrylate) (PBMA) can be leveraged to selectively skew the molecular weight distribution (MWD) and predictably alter the viscoelastic properties of blended PBMA mixtures. By mixing polymers with thermally active chain ends with polymers of different molecular weights and inactive chain ends, the MWD of the blends can be skewed high or low by selective depolymerization. This approach leads to the counterintuitive principle of "destructive strengthening" of a material. Finally, we demonstrate as a proof of concept the encryption of information within polymer mixtures by linking Morse code with the MWDs before and after selective depolymerization, allowing for encoding of data within blends of synthetic macromolecules.

INTRODUCTION

Reversible-deactivation radical polymerization (RDRP) techniques provide chain-end fidelity and enable control over chain length, polymer composition, and architecture.[1–11] RDRP methods also enable control over the breadth and skewness of polymer molecular weight distributions (MWD). In particular, Anastasaki,[12–16] Fors,[17–20] and Sumerlin[21,22] have demonstrated the precision engineering of dispersity ($Đ$) values and MWD skewness by approaches that include metered addition of initiator, tuning ligand concentration or initiator mixtures in ATRP, deliberate mixing of RAFT agents with disparate chain-transfer constants, and physical blending of polymers. These approaches are important because MWD shape and skewness govern many of the thermomechanical and viscoelastic properties of polymeric materials.[20,23–26] For example, polymer chains are susceptible to scission during mechanochemical recycling of thermoplastics, leading to a reduction in molecular weight.[27–29] However, in the particular scenario

where chain degradation leads to molecular weights below the chain-entanglement molecular weight (M_e), a reduction in physical entanglements within the polymer matrix leads to a dramatic loss of desirable thermomechanical properties. Chemical recycling by reversion to monomer is an alternative approach to overcome these recycling limitations. Recent innovations have shown that the active chain-ends of polymers generated by RDRP can be leveraged to initiate efficient depolymerization.[30–32]

Initial work on chain-end-initiated depolymerization relied on metal-catalyzed approaches to drive activation and depropagation of halogen-terminated polymers.[32,33] In addition to elevated temperatures, these systems required dilute conditions to overcome the high ceiling temperatures (T_c) innate to most vinyl polymers. Catalyst-free approaches have been employed to depolymerize thiocarbonylthio-terminated polymers by thermal[34–36] or photochemical activation of the dormant end-group at high temperatures and dilution.[37–39] Depolymerization of RDRP-generated polymers has more recently been extended to the bulk state, with rapid, solvent-free depolymerization of poly(methyl methyacrylate) (PMMA) occurring at temperatures well below those required for polymers without thermally sensitive chain ends.[40–43] Recent work has also demonstrated that phthalimide-based radical decarboxylations can drive efficient polymer degradation and depolymerization.[43–46] By conducting depolymerization under non-equilibrium conditions in which regenerated monomer is continuously removed, bulk depolymerization approaches may offer promise for large-scale adoption.[43] While these examples of chain-end initiated depolymerization have demonstrated the promise of RDRP techniques for generating polymers that are readily chemically recycled, depolymerization strategies have also emerged as a novel characterization tool for vinyl polymers.[47–49] However, there have been no reports of exploiting depolymerization as a method to reprogram polymer properties.

Recent work has demonstrated that strategic polymer deconstruction can counterintuitively improve material properties and allow skewing of MWDs.[50–52] Inspired by this, we hypothesized that polymer blends containing depolymerizable low molecular weight chains could be chemically recycled to skew the overall polymer MWD higher to generate products with enhanced viscoelastic properties, a result antithetical to conventional mechanochemical thermoplastic recycling (*vide supra*).

Herein, we employ an approach our group previously termed "skew customization by unzipping layered polymer traces" (SCULPT) that leverages selective depolymerization of RDRP-generated polymethacrylate blends to tune the MWD and viscoelastic properties of the resultant materials (Figure 1).[42] This strategy allows for the fabrication of thermoplastic materials possessing on-demand thermomechanical tunability triggered by a simple thermal stimulus. Furthermore, we explore how the SCULPT method can be leveraged to store or encode information within macromolecular materials, an emerging field within polymer science.[16,53–59] On this front, we took inspiration from the Junkers and Meier groups, who utilized the SEC traces from tailored molecular weight distributions[57,60] or sequence-defined macromolecules[58,59] to store data and represent outlines of images.

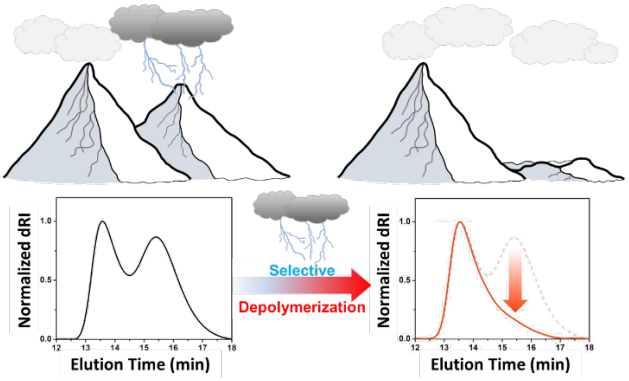

Figure 1. Demonstration of selective depolymerization which utilizes SCULPT methodology to skew molecular weight distributions and tune viscoelastic properties of polymer blends.

RESULTS AND DISCUSSION

Poly(butyl methacrylate) (PBMA) was selected as an example polymer to demonstrate the utility of the SCULPT approach. PBMA has a glass transition temperature (T_g) of ~25 °C,[61] which allows for facile compression molding at temperatures significantly lower than the trithiocarbonate (TTC)-initiated depolymerization onset temperature (145 °C).[37,40,42] We envisioned polymers with MWDs distinctly above or below M_e would demonstrate the most dramatic viscoelastic property shifts in blended materials following the SCULPT method. Thus, low molecular weight PBMA ($PBMA_{11k}$, M_n = 10.8 kg/mol, $Đ$ = 1.28) and high molecular weight PBMA ($PBMA_{64k}$, M_n = 63.8 kg/mol, $Đ$ = 1.14) samples were synthesized via photoiniferter methods.[1,62,63] We utilized our previously reported[42] difunctional chain-transfer agent, 1,3-dioxoisoindolin-2-yl 2-(((dodecylthio) carbonothioyl) thio)-2-methylpropanoate (Phth-TTC) to enable potential depolymerization from the α-end phthalimide ester (Phth) and ω-end TTC (Figures S1, S2). Depolymerization efficiency was quantified through thermogravimetric analysis (TGA) with $PBMA_{11k}$ and $PBMA_{64k}$ resulting in 89% and 81% depolymerization, respectively, following an isothermal hold at 250 °C for 100 min (Figures S3, S4).

Thermally stable PBMA of identical molecular weights were generated by removing both the Phth and TTC labile chain ends via aminolysis from $PBMA_{11k}$ and $PBMA_{64k}$ to yield end-group-removed (EGR) $PBMA_{11k,EGR}$ and $PBMA_{64k,EGR}$, respectively. Efficient removal of end-groups was confirmed by UV-vis detection during size exclusion chromatography (SEC) (Figure S5) and NMR spectroscopy

(Figure S6). A 50:50 wt% blend of depolymerizable $PBMA_{11k}$ and stable $PBMA_{64k,EGR}$ was prepared (Blend 1, M_n = 33.7 kg/mol, $Đ$ =1.70) (Figure 2A). We aimed to formulate Blend 1 to have $M_n \approx M_e$ ($M_{e,PBMA} \approx 38$ kg/mol)[61], and a monomodal PBMA sample of similar molecular weight, $PBMA_{31k}$ (M_n = 31.4 kg/mol, Đ =1.11), was synthesized for material comparisons (Figure S7). We then depolymerized Blend 1 by heating the bulk material under vacuum in a round bottom flask.[42] Blend 1 was heated to 250 °C for 1 h to yield a final polymer product with a MWD skewed higher and in close agreement with that of the stable $PBMA_{64k,EGR}$ (Skew High, M_n = 51.7 kg/mol, $Đ$ = 1.41) (Figure 2B).

Determining depolymerization efficiency by SEC generally requires the addition of a thermally stable internal standard.[36,38] However, since EGR-polymer traces remained unchanged through the duration of the experiment, we considered $PBMA_{64k,EGR}$ as an internal standard to compare to decreasing $PBMA_{11k}$ refractive index (RI) intensity. By SEC RI integration, Skew High demonstrated 84% depolymerization of depolymerizable material (Table S2). This correlated well to the 89% mass loss observed by TGA when the original (i.e., non-blended) $PBMA_{11k}$ was thermally treated. We also attempted to calculate a depolymerization efficiency from SEC deconvolution (Figures S8, S9). However, the Skew High material only contained trace amounts of $PBMA_{11k}$ and lacked a well-defined low molecular weight SEC peak for integration.

Skewing the MWD to lower molecular weights was achieved by preparing a similar 50:50 wt% blend with $PBMA_{11k,EGR}$ and depolymerizable $PBMA_{64k}$ (Blend 2, M_n = 33.9 kg/mol, $Đ$ = 1.68) (Figure 2C). Blend 2 was treated with an isothermal hold at 250 °C for 1 h to yield a final polymer distribution clearly skewed towards the lower end of the MWD, or $PBMA_{11k,EGR}$ (Skew Low, M_n = 17.3 kg/mol, $Đ$ = 1.99). 76% depolymerization of the $PBMA_{64k}$ being determined by deconvolution of the final SEC trace (Figure 2D, S10, S11). Interestingly, this efficiency of depolymerization is consistent with that determined for $PBMA_{64k}$ alone by TGA (81%) and RI integration (79%) (Table S2, Equation S2). These results demonstrate a successful post-polymerization methodology to skew MWDs above or below the chain entanglement molecular weight of PBMA ($M_e \approx 38$ kg/mol),[61] suggesting this approach could be useful to alter the properties of a polymer blend.

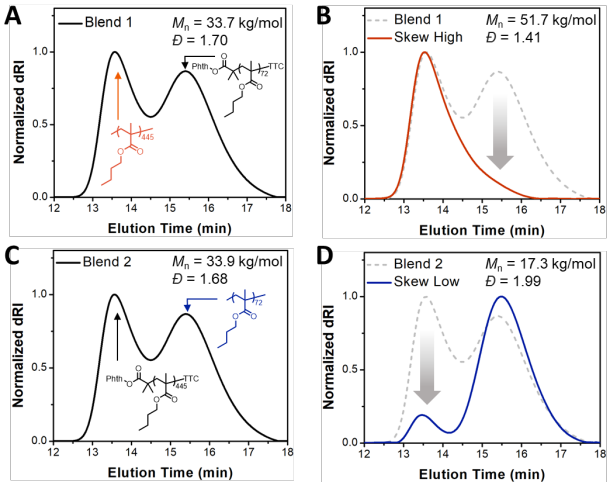

Figure 2. Size exclusion chromatography (SEC) traces of pre- and post-depolymerized PBMA blends. **A)** Blend 1 (50:50 wt% $PBMA_{64k}$: $PBMA_{11k,EGR}$, M_n = 33.7 kg/mol, $Đ$ = 1.70). **B)** Skew High MWD; Blend 1 after an isothermal hold at 250 °C for 1 h (M_n = 51.7 kg/mol, Đ = 1.41). **C)** Blend 2 (50:50 wt% $PBMA_{64k,EGR}$: $PBMA_{11k}$, M_n = 33.9 kg/mol, $Đ$ = 1.68). **D)** Skew Low MWD (i.e., Blend 2 after an isothermal hold at 250 °C for 1 h) (M_n = 17.3 kg/mol, $Đ$ = 1.99).

Table 1. Average molecular weights (M_n) and dispersities ($Đ$) of polymer molecular weight distributions in monomodal and blended PBMA samples.

Sample	*M_n (kg/mol)*	*$Đ$*
$PBMA_{11k}$	10.8	1.3
Skew Low	17.3	2.0
$PBMA_{31k}$	31.4	1.2
Blend 1	33.7	1.7
$PBMA_{64k}$	63.8	1.1
Skew High	51.7	1.4

We attempted dynamic mechanical analysis (DMA) for $PBMA_{11k}$, $PBMA_{64k}$, and Blend 1. Blend 1 expectedly showed a reduced level of the quasi-rubbery storage modulus of the material as compared to monomodal $PBMA_{64k}$ due to dilution of the entangled polymer distribution with the lower molecular weight polymer (Figure S12). $PBMA_{11k}$ specimens were highly sensitive to brittle fracture and could not be easily mounted on the DMA instrument, properties consistent with unentangled polymer materials.

The effect of depolymerization on viscoelastic properties was also investigated through shear rheology (Figure 3). Pre- and post-depolymerized blends were compared to monomodal PBMA samples with similar molecular weights during frequency sweep and creep-recovery experiments at 85 °C. Blends 1 and 2 were prepared on multi-gram scales and depolymerized at 250

°C to generate large batches of Skew High and Skew Low material, respectively. $PBMA_{11k}$, $PBMA_{64k}$, and Blend 1 were compression molded at 80 °C to yield clear, yellow disks. Post-depolymerized materials (Skew High and Skew Low blends) were purified and molded at 80 °C (Figure S13).

We then investigated the effect of MWD on the frequency dependence of the blended materials (Figures S14-20). Our first set of experiments involved frequency sweeps of Blend 1 being compared to a polymer with a monomodal MWD and similar M_n ($PBMA_{31k}$, M_n = 31.4 kg/mol, $Đ$ = 1.06) (Figure 3B). Given that $M_n \approx M_e$, $PBMA_{31k}$ approached a quasi-plateau yet still lacked a clear crossover of G' and G''. Interestingly, Blend 1 and $PBMA_{31k}$ showed almost identical curves, despite Blend 1 possessing 50 wt% of the polymer distribution significantly above M_e. Both samples functioned as viscoelastic liquids where G' approached G'' but lacked any crossover into a rubbery plateau regime. This can be explained by the majority of chains being largely below M_e, since a 50:50 wt% blend is still composed of a vast majority of low MW chains. Frequency sweeps were then measured for the Skew Low material and $PBMA_{11k}$, both of which had $M_n < M_e$. The Skew Low material behaved as a viscoelastic liquid with the loss modulus (G'') dominating storage modulus (G') at all frequencies, nearly identical to its monomodal counterpart $PBMA_{11k}$. The similarity in frequency sweeps indicates an efficient transformation in viscoelastic properties despite incomplete (~80%) depolymerization of the $PBMA_{64k}$ component (Figure 3A). However, the high MW component had a profound effect on the creep susceptibility of the material in comparison to the monomodal counterpart, despite their highly similar frequency-dependent behavior (*vide infra*).

As anticipated, the Skew High material behaved as a viscoelastic solid with a distinct crossover of G' and G'' into a rubbery plateau regime (Figure 3C). This matches the expected viscoelastic behavior of an entangled polymer melt, given that $M_n > M_e$ (Table S3, Equation S1). As such, the viscoelastic skewing was proven to be highly efficient, with near identical frequency sweep curves as the monomodal $PBMA_{64k}$. This supports our hypothesis that utilizing depolymerization as a recycling strategy can potentially enable destructive *strengthening* of a material. It is also noteworthy that the Skew High material and $PBMA_{64k}$ showed greater similarities to one another in their G' and G'' traces, as compared to those shown from the Skew Low material and $PBMA_{11k}$. This phenomenon is expected given that $PBMA_{11k}$ depolymerizes to a greater extent (91%) than $PBMA_{64k}$ (82%). These results demonstrate the ability to predictably shift macromolecular properties to dramatically alter the flow behavior of thermoplastic materials.

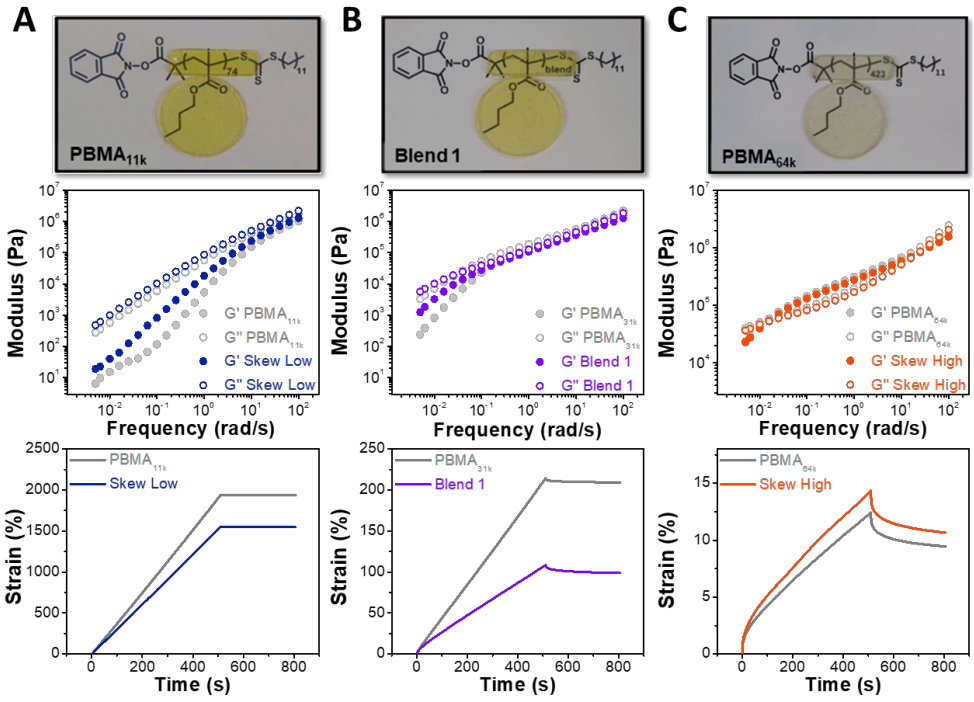

Figure 3. Images of compression molded PBMA specimens (top row) with associated frequency sweeps (middle row) and creep-recovery experiments (bottom row), comparing skewed or blended material with monomodal PBMA counterparts. Frequency dependence experiments were run at 85 °C with 0.3% oscillatory strain. Creep-recovery experiments were run at 85 °C with 2.5 kPa stress and 0.3% strain. **(A)** Skew Low material and $PBMA_{11k}$ with $M_n < M_e$ exhibit the least resistance to creep and no recovery. **(B)** Blend 1 and $PBMA_{31k}$ with $M_n \approx M_e$ show moderate strain with near-linear stress deformation and a low level of recovery. **(C)** Skew High and $PBMA_{64k}$ with $M_n > M_e$ exhibit viscoelastic solid behavior with $\tan(\delta)_{min} < 1$, the greatest resistance to creep, and the highest recovery.

Creep-recovery experiments were then conducted for the $PBMA_{11k}$, $PBMA_{31k}$, and $PBMA_{64k}$ monomodal MWDs as well as Blend 1, Skew Low, and Skew High samples (Figure 3, S21). Below M_e, the $PBMA_{11k}$ and Skew Low materials showed significant viscous creep deformation and no elastic recovery (< 0.3%) (Figure 3A), which was consistent with the findings from frequency sweep measurements that suggested these polymers were unentangled in the melt. At $M_n \approx M_e$, $PBMA_{31k}$ and Blend 1 showed significantly decreased creep deformation as compared to the low MW PBMA samples but maintained low elastic recovery (Figure 3B). While frequency sweeps of the $PBMA_{31k}$ and Blend 1 samples were comparable, Blend 1 displayed significantly lower viscous deformation than that of $PBMA_{31k}$ (109% versus 214%), as well as a slight increase in elastic recovery. The higher recovery and lower viscous creep observed in Blend 1 is attributed to the presence of entanglements within the higher molecular weight chains of the $PBMA_{64k}$ component.[64]

Table 2. Polymer molecular weight distribution and resulting mechanical properties.

Sample	*M_n vs M_e*	*tan (δ)*	*Strain %*	*Recovery %*
$PBMA_{11k}$	$M_n < M_e$	> 1	1940	< 0.3
Skew Low	$M_n < M_e$	> 1	1554	< 0.3
$PBMA_{31k}$	$M_n \approx M_e$	≈ 1	214	2
Blend 1	$M_n \approx M_e$	≈ 1	109	9
$PBMA_{64k}$	$M_n > M_e$	< 1	12	25
Skew High	$M_n > M_e$	< 1	14	21

As expected, the $PBMA_{64k}$ and Skew High samples with $M_n > M_e$ exhibited the greatest creep resistance (12-14% viscous deformation) and greatest recovery (21-25%) (Figure 3C). In both frequency sweep and creep-recovery studies, the flow properties of Skew High and Skew Low materials compared well to their virgin, monomodal counterparts. The resemblance in elastic and viscous moduli as well as their creep deformation/recovery indicate that depolymerized materials and virgin polymers with similar MWDs have similar rheological properties. These findings suggest that this approach to thermal depolymerization does not compromise the macromolecular properties of thermally stable polymers and offers a viable route towards on-demand selective skewing of polymer properties.

While it has recently been demonstrated that controlled depolymerization can lead to a gradual reduction in polymer molecular weight[48], one noteworthy aspect of the chain-end-initiated depolymerization process reported here is the vertical depression of polymer peaks observed in SEC rather than shifts towards lower molecular weights. Upon generating a chain-end radical, rapid and near-complete depolymerization to monomer, small molecule RAFT agents, or oligomers occurs.[65] By avoiding the generation of partially-depolymerized chains or coupled products, we circumvent the emergence of new polymer signals in SEC. We envisioned that this aspect of RDRP chain-end-initiated depolymerization could be leveraged to encode messaging via selective depolymerization in polymer blends.

While binary has been the dominant form of macromolecular information storage[53,55,56], we determined that Morse code would be the most straightforward translation of SCULPTed polymer blends. As such, we chose a dot (•) to represent an unfunctionalized PMMA distribution exhibiting no peak intensity change after depolymerization, while a dash (—) is signaled by a peak depression (i.e., depolymerized polymer distribution). We chose to encode the straightforward message of "PMMA" after depolymerization, as it requires at most a quaternary blend. Four polymer blends were prepared with depolymerizable MWDs to yield final MWDs that revealed the desired Morse code message (Figure 4). Peak depressions could be seen in all four samples, thus allowing for deconvolution of the encoded message. Blend 3 contained two internal, depolymerizable distributions that underwent depression after an isothermal hold at 250 °C to yield "•——•" (P) (Figure 4, Table S1). Similar thermal treatment to blends 4, 5, and 6 also resulted in depressions to reveal "—" (M), "—" (M), and "•—" (A) (Figures 4, Table S1). To further demonstrate the potential for encryption (e.g., if incorrect blend sequencing was used to construct the message), alternative blends were made that yielded similar SEC traces but revealed different letters after thermal treatment. For example, Blend 2 depolymerizes to yield "—•" (N) while Blend 7 contained solely unfunctionalized material, thus resisting depolymerization to yield "••" (I) (Figure S22 and Figure S23). This demonstrates that effectively indistinguishable SEC traces can reveal cryptographically distinct polymer MWDs (e.g. different Morse code lettering from an "identical" blend) after thermal treatment, allowing for another degree of message encryption. This preliminary information storage platform further demonstrates how bulk depolymerization can have utility beyond chemical recycling and tuning of macromolecular properties.

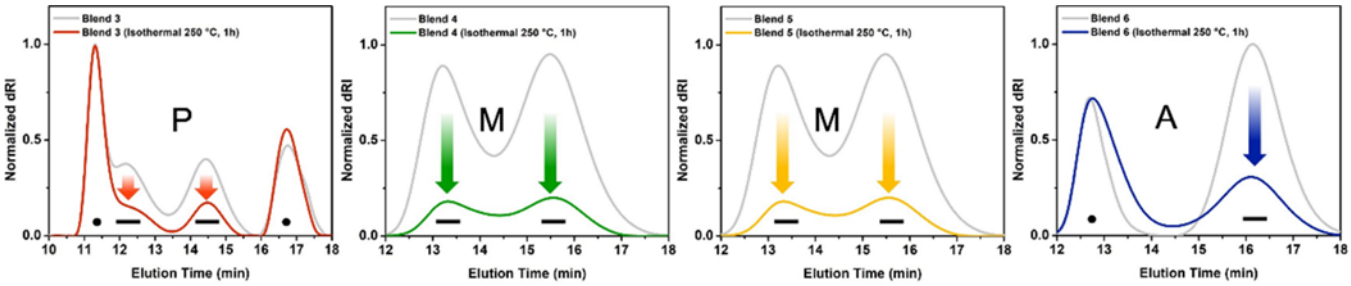

Figure 4. Morse code messaging through selective peak depolymerization in polymer blends. Unfunctionalized distributions exhibiting no peak intensity change after depolymerization represent a dot (•), while peak depression during depolymerization represents a dash (—). Blend 3 depolymerizes to reveal the letter "P" (•——•). Blends 4 and 5 depolymerize to reveal the letter "M" (——). Blend 6 depolymerizes to reveal the letter "A" (•—). All blends were held at 250 °C for 1 h to selectively depolymerize Phth-PMMA-TTC distributions. All samples were normalized to the unfunctionalized distributions, except for Blends 4 and 5, which were normalized to the solvent peak at elution. For blend compositions, see Table S1.

CONCLUSION

This study demonstrates that chain-end reactivation of polymers prepared by reversible-deactivation radical polymerization (RDRP) facilitates the selective depolymerization of polymer blends. By employing the SCULPT method, we achieved precise modifications in the polymer blends, significantly altering their thermomechanical properties. Notably, Blend 1, which initially exhibited viscoelastic liquid characteristics, was converted into a blend displaying predominantly viscoelastic solid-like behavior. Additionally, the methodology effectively reduced the average molecular weight, resulting in materials with enhanced plasticity. This strategy could be leveraged to investigate the effect of destructive skewing on blends comprised of entirely different polymers rather than identical polymers with distinct MWDs, potentially enabling translation to mixed polymer waste streams.

Our approach also introduced a novel concept of data encryption within polymer blends, utilizing selective depolymerization to encode and later reveal messages, thereby offering potential for secure data transmission. These findings deepen our understanding of the impact of chain-end dynamics on material properties and enable the development of responsive polymers with applications in smart materials and information technology.

ACKNOWLEDGEMENTS

This work was supported as part of the Center for Plastics Innovation, an Energy Frontier Research Center funded by the U.S. Department of Energy, Office of Science, Basic Energy Sciences at the University of Delaware under award # DE-SC0021166.

REFERENCES

(1) Hartlieb, M. Photo-Iniferter RAFT Polymerization. *Macromol. Rapid Commun.* **2022**, *43* (1), 2100514. https://doi.org/10.1002/marc.202100514.

(2) Lehnen, A.-C.; M. Kurki, J. A.; Hartlieb, M. The Difference between Photo-Iniferter and Conventional RAFT Polymerization: High Livingness Enables the Straightforward Synthesis of Multiblock Copolymers. *Polym. Chem.* **2022**, *13* (11), 1537–1546. https://doi.org/10.1039/D1PY01530C.

(3) Chen, M.; Zhong, M.; Johnson, J. A. Light-Controlled Radical Polymerization: Mechanisms, Methods, and Applications. *Chem. Rev.* **2016**, *116* (17), 10167–10211. https://doi.org/10.1021/acs.chemrev.5b00671.

(4) Hill, M. R.; Carmean, R. N.; Sumerlin, B. S. Expanding the Scope of RAFT Polymerization: Recent Advances and New Horizons. *Macromolecules* **2015**, *48* (16), 5459–5469. https://doi.org/10.1021/acs.macromol.5b00342.

(5) Perrier, S. 50th Anniversary Perspective: RAFT Polymerization—A User Guide. *Macromolecules* **2017**, *50* (19), 7433–7447. https://doi.org/10.1021/acs.macromol.7b00767.

(6) Bowman, J. I.; Eades, C. B.; Korpanty, J.; Garrison, J. B.; Scheutz, G. M.; Goodrich, S. L.; Gianneschi, N. C.; Sumerlin, B. S. Controlling Morphological Transitions of Polymeric Nanoparticles via Doubly Responsive Block Copolymers. *Macromolecules* **2023**, *56* (9), 3316–3323. https://doi.org/10.1021/acs.macromol.3c00445.

(7) Garrison, J. B.; Hughes, R. W.; Young, J. B.; Sumerlin, B. S. Photoinduced SET to Access Olefin-Acrylate Copolymers. *Polym. Chem.* **2022**, *13* (7), 982–988. https://doi.org/10.1039/D1PY01643A.

(8) Benaglia, M.; Rizzardo, E.; Alberti, A.; Guerra, M. Searching for More Effective Agents and Conditions for the RAFT Polymerization of MMA: Influence of Dithioester Substituents, Solvent, and Temperature. *Macromolecules* **2005**, *38* (8), 3129–3140. https://doi.org/10.1021/ma0480650.

(9) Xu, J.; Shanmugam, S.; Fu, C.; Aguey-Zinsou, K.-F.; Boyer, C. Selective Photoactivation: From a Single Unit Monomer Insertion Reaction to Controlled Polymer Architectures. *J. Am. Chem. Soc.* **2016**, *138* (9), 3094–3106. https://doi.org/10.1021/jacs.5b12408.

(10) Roy, D.; Ullah, A.; Sumerlin, B. S. Rapid Block Copolymer Synthesis by Microwave-Assisted RAFT Polymerization. *Macromolecules* **2009**, *42* (20), 7701–7708. https://doi.org/10.1021/ma901471k.

(11) Golas, P. L.; Tsarevsky, N. V.; Sumerlin, B. S.; Walker, L. M.; Matyjaszewski, K. Multisegmented Block Copolymers by 'Click' Coupling of Polymers Prepared

by ATRP. *Aust. J. Chem.* **2007**, *60* (6), 400–404. https://doi.org/10.1071/CH07073.
(12) Whitfield, R.; Parkatzidis, K.; Truong, N. P.; Junkers, T.; Anastasaki, A. Tailoring Polymer Dispersity by RAFT Polymerization: A Versatile Approach. *Chem* **2020**, *6*, 1340–1352. https://doi.org/doi.org/10.1016/j.chempr.2020.04.020.
(13) Shimizu, T.; Truong, N. P.; Whitfield, R.; Anastasaki, A. Tuning Ligand Concentration in Cu(0)-RDRP: A Simple Approach to Control Polymer Dispersity. *ACS Polym. Au* **2021**, *1* (3), 187–195. https://doi.org/10.1021/acspolymersau.1c00030.
(14) Parkatzidis, K.; P. Truong, N.; Nefeli Antonopoulou, M.; Whitfield, R.; Konkolewicz, D.; Anastasaki, A. Tailoring Polymer Dispersity by Mixing Chain Transfer Agents in PET-RAFT Polymerization. *Polym. Chem.* **2020**, *11* (31), 4968–4972. https://doi.org/10.1039/D0PY00823K.
(15) Whitfield, R.; Truong, N. P.; Anastasaki, A. Precise Control of Both Dispersity and Molecular Weight Distribution Shape by Polymer Blending. *Angew. Chem.* **2021**, *133* (35), 19532–19537. https://doi.org/10.1002/ange.202106729.
(16) Antonopoulou, M.-N.; Whitfield, R.; Truong, N. P.; Wyers, D.; Harrisson, S.; Junkers, T.; Anastasaki, A. Concurrent Control over Sequence and Dispersity in Multiblock Copolymers. *Nat. Chem.* **2022**, *14* (3), 304–312. https://doi.org/10.1038/s41557-021-00818-8.
(17) Gentekos, D. T.; Sifri, R. J.; Fors, B. P. Controlling Polymer Properties through the Shape of the Molecular-Weight Distribution. *Nat. Rev. Mater.* **2019**, *4* (12), 761–774. https://doi.org/10.1038/s41578-019-0138-8.
(18) I. Rosenbloom, S.; J. Sifri, R.; P. Fors, B. Achieving Molecular Weight Distribution Shape Control and Broad Dispersities Using RAFT Polymerizations. *Polym. Chem.* **2021**, *12* (34), 4910–4915. https://doi.org/10.1039/D1PY00399B.
(19) Sifri, R. J.; Padilla-Vélez, O.; Coates, G. W.; Fors, B. P. Controlling the Shape of Molecular Weight Distributions in Coordination Polymerization and Its Impact on Physical Properties. *J. Am. Chem. Soc.* **2020**, *142* (3), 1443–1448. https://doi.org/10.1021/jacs.9b11462.
(20) Rosenbloom, S. I.; Fors, B. P. Shifting Boundaries: Controlling Molecular Weight Distribution Shape for Mechanically Enhanced Thermoplastic Elastomers. *Macromolecules* **2020**, *53* (17), 7479–7486. https://doi.org/10.1021/acs.macromol.0c00954.
(21) Hill, M. R.; MacKrell, E. J.; Forsthoefel, C. P.; Jensen, S. P.; Chen, M.; Moore, G. A.; He, Z. L.; Sumerlin, B. S. Biodegradable and pH-Responsive Nanoparticles Designed for Site-Specific Delivery in Agriculture. *Biomacromolecules* **2015**, *16* (4), 1276–1282. https://doi.org/10.1021/acs.biomac.5b00069.
(22) P. Easterling, C.; Kubo, T.; M. Orr, Z.; E. Fanucci, G.; S. Sumerlin, B. Synthetic Upcycling of Polyacrylates through Organocatalyzed Post-Polymerization Modification. *Chem. Sci.* **2017**, *8* (11), 7705–7709. https://doi.org/10.1039/C7SC02574B.
(23) Matyjaszewski, K. Atom Transfer Radical Polymerization: From Mechanisms to Applications. *Isr. J. Chem.* **2012**, *52* (3–4), 206–220. https://doi.org/10.1002/ijch.201100101.
(24) I. Rosenbloom, S.; T. Gentekos, D.; N. Silberstein, M.; P. Fors, B. Tailor-Made Thermoplastic Elastomers: Customisable Materials via Modulation of Molecular Weight Distributions. *Chem. Sci.* **2020**, *11* (5), 1361–1367. https://doi.org/10.1039/C9SC05278J.
(25) Lessard, J. J.; Stewart, K. A.; Sumerlin, B. S. Controlling Dynamics of Associative Networks through Primary Chain Length. *Macromolecules* **2022**, *55* (22), 10052–10061. https://doi.org/10.1021/acs.macromol.2c01909.
(26) Doi, M.; Edwards, S. F.; Edwards, S. F. *The Theory of Polymer Dynamics*; Clarendon Press, 1988.
(27) Schyns, Z. O. G.; Shaver, M. P. Mechanical Recycling of Packaging Plastics: A Review. *Macromol. Rapid Commun.* **2021**, *42* (3), 2000415. https://doi.org/10.1002/marc.202000415.
(28) Ragaert, K.; Delva, L.; Van Geem, K. Mechanical and Chemical Recycling of Solid Plastic Waste. *Waste Manag.* **2017**, *69*, 24–58. https://doi.org/10.1016/j.wasman.2017.07.044.
(29) Hinton, Z. R.; Talley, M. R.; Kots, P. A.; Le, A. V.; Zhang, T.; Mackay, M. E.; Kunjapur, A. M.; Bai, P.; Vlachos, D. G.; Watson, M. P.; Berg, M. C.; Epps, T. H.; Korley, L. T. J. Innovations Toward the Valorization of Plastics Waste. *Annu. Rev. Mater. Res.* **2022**, *52* (1), 249–280. https://doi.org/10.1146/annurev-matsci-081320-032344.
(30) Carmean, R. N.; Figg, C. A.; Scheutz, G. M.; Kubo, T.; Sumerlin, B. S. Catalyst-Free Photoinduced End-Group Removal of Thiocarbonylthio Functionality. *ACS Macro Lett.* **2017**, *6* (2), 185–189. https://doi.org/10.1021/acsmacrolett.7b00038.
(31) Deng, Z.; Gillies, E. R. Emerging Trends in the Chemistry of End-to-End Depolymerization. *JACS Au* **2023**, *3* (9), 2436–2450. https://doi.org/10.1021/jacsau.3c00345.
(32) Jones, G. R.; Wang, H. S.; Parkatzidis, K.; Whitfield, R.; Truong, N. P.; Anastasaki, A. Reversed Controlled Polymerization (RCP): Depolymerization from Well-Defined Polymers to Monomers. *J. Am. Chem. Soc.* **2023**, *145* (18), 9898–9915. https://doi.org/10.1021/jacs.3c00589.
(33) Sano, Y.; Konishi, T.; Sawamoto, M.; Ouchi, M. Controlled Radical Depolymerization of Chlorine-Capped PMMA via Reversible Activation of the Terminal Group by Ruthenium Catalyst. *Eur. Polym. J.* **2019**, *120*, 109181. https://doi.org/10.1016/j.eurpolymj.2019.08.008.
(34) Martinez, M. R.; Dadashi-Silab, S.; Lorandi, F.; Zhao, Y.; Matyjaszewski, K. Depolymerization of P(PDMS11MA) Bottlebrushes via Atom Transfer Radical Polymerization with Activator Regeneration. *Macromolecules* **2021**, *54* (12), 5526–5538. https://doi.org/10.1021/acs.macromol.1c00415.
(35) J. Flanders, M.; M. Gramlich, W. Reversible-Addition Fragmentation Chain Transfer (RAFT) Mediated Depolymerization of Brush Polymers. *Polym. Chem.* **2018**, *9* (17), 2328–2335. https://doi.org/10.1039/C8PY00446C.
(36) Wang, H. S.; Truong, N. P.; Pei, Z.; Coote, M. L.; Anastasaki, A. Reversing RAFT Polymerization: Near-Quantitative Monomer Generation Via a Catalyst-Free Depolymerization Approach. *J. Am. Chem. Soc.* **2022**, *144* (10), 4678–4684. https://doi.org/10.1021/jacs.2c00963.
(37) Wang, H. S.; Truong, N. P.; Jones, G. R.; Anastasaki, A. Investigating the Effect of End-Group, Molecular Weight, and Solvents on the Catalyst-Free Depolymerization of RAFT Polymers: Possibility to Reverse the Polymerization of Heat-Sensitive Polymers. *ACS Macro Lett.* **2022**, *11* (10), 1212–1216. https://doi.org/10.1021/acsmacrolett.2c00506.
(38) Young, J. B.; Bowman, J. I.; Eades, C. B.; Wong, A. J.; Sumerlin, B. S. Photoassisted Radical Depolymerization. *ACS Macro Lett.* **2022**, *11* (12), 1390–1395. https://doi.org/10.1021/acsmacrolett.2c00603.

(39) Bellotti, V.; Parkatzidis, K.; Suk Wang, H.; Watuthanthrige, N. D. A.; Orfano, M.; Monguzzi, A.; P. Truong, N.; Simonutti, R.; Anastasaki, A. Light-Accelerated Depolymerization Catalyzed by Eosin Y. *Polym. Chem.* **2023**, *14* (3), 253–258. https://doi.org/10.1039/D2PY01383E.

(40) De Luca Bossa, F.; Yilmaz, G.; Matyjaszewski, K. Fast Bulk Depolymerization of Polymethacrylates by ATRP. *ACS Macro Lett.* **2023**, *12* (8), 1173–1178. https://doi.org/10.1021/acsmacrolett.3c00389.

(41) Whitfield, R.; Jones, G. R.; Truong, Nghia. P.; Manring, L. E.; Anastasaki, A. Solvent-Free Chemical Recycling of Polymethacrylates Made by ATRP and RAFT Polymerization: High-Yielding Depolymerization at Low Temperatures. *Angew. Chem.* **2023**, *135* (38), e202309116. https://doi.org/10.1002/ange.202309116.

(42) Young, J. B.; Hughes, R. W.; Tamura, A. M.; Bailey, L. S.; Stewart, K. A.; Sumerlin, B. S. Bulk Depolymerization of Poly(Methyl Methacrylate) via Chain-End Initiation for Catalyst-Free Reversion to Monomer. *Chem e202309116*. https://doi.org/10.1002/anie.202309116.

(43) Hughes, R. W.; Lott, M. E.; Zastrow, I. S.; Young, J. B.; Maity, T.; Sumerlin, B. S. Bulk Depolymerization of Methacrylate Polymers via Pendent Group Activation. *J. Am. Chem. Soc.* **2024**, *146* (9), 6217–6224. https://doi.org/10.1021/jacs.3c14179.

(44) Anyaegbu, C.; Vidali, G.; Haridas, D.; Hooper, J. F. Radical Decarboxylation: An Emerging Tool in Polymer Synthesis. *Polym. Chem.* **2024**, *15* (25), 2537–2547. https://doi.org/10.1039/D4PY00267A.

(45) Young, J. B.; Goodrich, S. L.; Lovely, J. A.; Ross, M. E.; Bowman, J. I.; Hughes, R. W.; Sumerlin, B. S. Mechanochemically Promoted Functionalization of Postconsumer Poly(Methyl Methacrylate) and Poly(α-Methylstyrene) for Bulk Depolymerization. *Angew. Chem. Int. Ed. n/a* (n/a), e202408592. https://doi.org/10.1002/anie.202408592.

(46) Hughes, R. W.; Marquez, J. D.; Young, J. B.; Garrison, J. B.; Zastrow, I. S.; Evans, A. M.; Sumerlin, B. S. Selective Electrochemical Modification and Degradation of Polymers. *Angew. Chem. Int. Ed.* **2024**, *63* (20), e202403026. https://doi.org/10.1002/anie.202403026.

(47) Parkatzidis, K.; Wang, H. S.; Anastasaki, A. Photocatalytic Upcycling and Depolymerization of Vinyl Polymers. *Angew. Chem.* **2024**, *136* (19), e202402436. https://doi.org/10.1002/ange.202402436.

(48) Wang, H. S.; Parkatzidis, K.; Junkers, T.; Truong, N. P.; Anastasaki, A. Controlled Radical Depolymerization: Structural Differentiation and Molecular Weight Control. *Chem* **2024**, *10* (1), 388–401. https://doi.org/10.1016/j.chempr.2023.09.027.

(49) Yu, H.; Liu, L.; Yin, R.; Jayapurna, I.; Wang, R.; Xu, T. Mapping Composition Evolution through Synthesis, Purification, and Depolymerization of Random Heteropolymers. *J. Am. Chem. Soc.* **2024**, *146* (9), 6178–6188. https://doi.org/10.1021/jacs.3c13909.

(50) Wang, Z.; Zheng, X.; Ouchi, T.; Kouznetsova, T. B.; Beech, H. K.; Av-Ron, S.; Matsuda, T.; Bowser, B. H.; Wang, S.; Johnson, J. A.; Kalow, J. A.; Olsen, B. D.; Gong, J. P.; Rubinstein, M.; Craig, S. L. Toughening Hydrogels through Force-Triggered Chemical Reactions That Lengthen Polymer Strands. *Science* **2021**, *374* (6564), 193–196. https://doi.org/10.1126/science.abg2689.

(51) Wang, S.; Hu, Y.; Kouznetsova, T. B.; Sapir, L.; Chen, D.; Herzog-Arbeitman, A.; Johnson, J. A.; Rubinstein, M.; Craig, S. L. Facile Mechanochemical Cycloreversion of Polymer Cross-Linkers Enhances Tear Resistance. *Science* **2023**, *380* (6651), 1248–1252. https://doi.org/10.1126/science.adg3229.

(52) Kim, Y.; Kim, C. Tailoring Molecular Weight Distribution via Polymer Degradability. *Polym. Chem.* **2024**, *15* (3), 166–171. https://doi.org/10.1039/D3PY01153D.

(53) Soete, M.; Mertens, C.; Badi, N.; Du Prez, F. E. Reading Information Stored in Synthetic Macromolecules. *J. Am. Chem. Soc.* **2022**, *144* (49), 22378–22390. https://doi.org/10.1021/jacs.2c10316.

(54) Chan-Seng, D.; Zamfir, M.; Lutz, J.-F. Polymer-Chain Encoding: Synthesis of Highly Complex Monomer Sequence Patterns by Using Automated Protocols. *Angew. Chem.* **2012**, *124* (49), 12420–12423. https://doi.org/10.1002/ange.201206371.

(55) Al Ouahabi, A.; Charles, L.; Lutz, J.-F. Synthesis of Non-Natural Sequence-Encoded Polymers Using Phosphoramidite Chemistry. *J. Am. Chem. Soc.* **2015**, *137* (16), 5629–5635. https://doi.org/10.1021/jacs.5b02639.

(56) Roy, R. K.; Meszynska, A.; Laure, C.; Charles, L.; Verchin, C.; Lutz, J.-F. Design and Synthesis of Digitally Encoded Polymers That Can Be Decoded and Erased. *Nat. Commun.* **2015**, *6* (1), 7237. https://doi.org/10.1038/ncomms8237.

(57) Junkers, T. Polymers in the Blender. *Macromol. Chem. Phys.* **2020**, *221* (18), 2000234. https://doi.org/10.1002/macp.202000234.

(58) Solleder, S. C.; Schneider, R. V.; Wetzel, K. S.; Boukis, A. C.; Meier, M. A. R. Recent Progress in the Design of Monodisperse, Sequence-Defined Macromolecules. *Macromol. Rapid Commun.* **2017**, *38* (9), 1600711. https://doi.org/10.1002/marc.201600711.

(59) Boukis, A. C.; Meier, M. A. R. Data Storage in Sequence-Defined Macromolecules *via* Multicomponent Reactions. *Eur. Polym. J.* **2018**, *104*, 32–38. https://doi.org/10.1016/j.eurpolymj.2018.04.038.

(60) H. Vrijsen, J.; Rubens, M.; Junkers, T. Simple and Secure Data Encryption via Molecular Weight Distribution Fingerprints. *Polym. Chem.* **2020**, *11* (40), 6463–6470. https://doi.org/10.1039/D0PY01071E.

(61) Stetsyshyn, Y.; Raczkowska, J.; Lishchynskyi, O.; Awsiuk, K.; Zemla, J.; Dąbczyński, P.; Kostruba, A.; Harhay, K.; Ohar, H.; Orzechowska, B.; Panchenko, Y.; Vankevych, P.; Budkowski, A. Glass Transition in Temperature-Responsive Poly(Butyl Methacrylate) Grafted Polymer Brushes. Impact of Thickness and Temperature on Wetting, Morphology, and Cell Growth. *J. Mater. Chem. B* **2018**, *6* (11), 1613–1621. https://doi.org/10.1039/C8TB00088C.

(62) Carmean, R. N.; Sims, M. B.; Figg, C. A.; Hurst, P. J.; Patterson, J. P.; Sumerlin, B. S. Ultrahigh Molecular Weight Hydrophobic Acrylic and Styrenic Polymers through Organic-Phase Photoiniferter-Mediated Polymerization. *ACS Macro Lett.* **2020**, *9* (4), 613–618. https://doi.org/10.1021/acsmacrolett.0c00203.

(63) Olson, R. A.; Lott, M. E.; Garrison, J. B.; Davidson, C. L. G. I.; Trachsel, L.; Pedro, D. I.; Sawyer, W. G.; Sumerlin, B. S. Inverse Miniemulsion Photoiniferter Polymerization for the Synthesis of Ultrahigh Molecular Weight Polymers. *Macromolecules* **2022**, *55* (19), 8451–8460. https://doi.org/10.1021/acs.macromol.2c01239.

(64) Zosel, A. Rheological Properties of Disperse Systems at Low Shear Stresses. *Rheol. Acta* **1982**, *21* (1), 72–80. https://doi.org/10.1007/BF01520707.

(65) Häfliger, F.; Truong, N. P.; Wang, H. S.; Anastasaki, A. Fate of the RAFT End-Group in the Thermal Depolymerization of Polymethacrylates. *ACS Macro Lett.* **2023**, *12* (9), 1207–1212. https://doi.org/10.1021/acsmacrolett.3c00418.